

# **Influence of reaction times and anticipation on the stability of vehicular traffic flow**

Martin Treiber, Dr. (corresponding author)  
Institute for Transport & Economics  
Technische Universität Dresden  
Andreas-Schubert-Straße 23  
D-01062 Dresden, Germany  
phone: +49 351 463 36794  
fax: +49 351 463 36809  
treiber@vwi.tu-dresden.de

Arne Kesting, Dipl.-Phys.  
Institute for Transport & Economics  
Technische Universität Dresden  
Andreas-Schubert-Straße 23  
D-01062 Dresden, Germany  
phone: +49 351 463 36838  
fax: +49 351 463 36809  
kesting@vwi.tu-dresden.de

Dirk Helbing, Prof. Dr.  
Institute for Transport & Economics  
Technische Universität Dresden  
Andreas-Schubert-Straße 23  
D-01062 Dresden, Germany  
phone: +49 351 463 36802  
fax: +49 351 463 36809  
helbing@vwi.tu-dresden.de

Figures and Tables: 5+1  
Revision date: November 15, 2006  
Converted from Latex to Word: March 26, 2007

**ABSTRACT**

We investigate two causes for the instability of traffic flow: The time lag caused by finite accelerations of the vehicles, and the delay caused by the finite reaction times of the drivers. Furthermore, we simulate to which degree drivers may compensate for these delays by looking several vehicles ahead and anticipate future traffic situations. Since vehicular traffic flow is an extended multi-particle system with many degrees of freedom, two concepts of linear stability have to be considered: Local stability of a car following a leader that drives at constant velocity, and string (chain) stability of a ‘platoon’ of several vehicles following each other. Typically, string stability is a much more restrictive criterion than local stability. We simulate both types of stability with the Human Driver Model [M. Treiber *et al.*, *Physica A*, Vol. 360 (1), 71-88 (2006)], which includes all the features above. We found several interesting results: (i) with a suitable anticipation, we obtained string stability for reaction times exceeding the safety time gap, which, to our knowledge, has not yet been obtained for any other car-following model; (ii) parameter changes that destabilize the model variant with zero reaction time may stabilize the model with finite reaction times and vice versa, (iii) distributed reaction times (every driver has a different reaction time) can stabilize the system compared to drivers with identical reaction times that are equal to the mean.

## INTRODUCTION

Modelling of human driving behavior is a controversial topic in traffic science (1,2,3). It is obvious, however, that an essential feature of human (in contrast to automated) drivers is a considerable reaction time, which is a consequence of the physiological aspects of sensing, perceiving, deciding, and performing an action (4). This complex reaction time  $T'$  is of the order of 1.2 s (5). In addition, it varies strongly between different drivers (age, gender), different stimuli, and different studies (cf. the review of human perception-brake reaction time studies (5)).

Remarkably, in dense (not yet congested) traffic, the modal value in the time gap distribution (which is the most probable value) on Dutch or German freeways are around 0.9 s (6,7), i.e., *below* the average value of the reaction time. This has to be compared with the linear stability results of simple car-following models which become unstable if the reaction time exceeds half the value of the time gap (8,9). In such models, the acceleration depends, in general, on the own velocity, and the distance and velocity difference to the previous vehicle which are the input variables of automated driving systems, sometimes called 'adaptive cruise control' (ACC) (11,12). Reaction times are most commonly modelled by introducing a dead time (time delay)  $T'$  between the accelerating or braking action of the driver, and the input stimuli to which a driver reacts (8,12,13).

Clearly, human drivers take into account more input variables to overcome the stability limit mentioned above. For example, unlike machines, human drivers routinely scan the traffic situation several vehicles ahead and anticipate future traffic situations leading, in turn, to an increased stability.

The different stabilizing and destabilizing factors of the driver's behavior and the vehicle dynamics constitute a nonlinear feedback control system and can be visualized in a flow diagram (Fig. 1). The instability of traffic flow is caused by the delay the system needs to respond to a certain action of a controller (14,15). More specifically, the controllers are the drivers, the quantity to be controlled is the velocity of the own vehicle (or the distance to the preceding vehicle), the input stimuli are the observed distances and velocities, respectively, and the actions to reach desired velocities or distances consist in accelerating or braking (we do not consider lane changes here). The task of following a single vehicle can be modelled by a nonlinear controller containing a gain function (i.e., a car-following model without delay), and a dead-time or delay element. Since only the accelerations can be controlled, the control path contains one or two additional integrative elements. To include anticipation, additional (nonlinear) derivative elements are incorporated into the control path.

For determining the *linear local stability*, one can apply standard methods of control theory to the linearized system yielding an upper limit of the reaction time  $T'$ , which decreases with the sensitivity of the car-following model, i.e., how much it accelerates (decelerates) if the actual distance is too large (small). However, it is well known in traffic theory for car-following models with zero reaction time (16,3), and also for macroscopic models (17), that small sensitivities (acceleration capabilities) *increase* the linear string instability if a platoon of *several* vehicles is considered, i.e., the perturbations will amplify while propagating downstream the chain of vehicles. Typically, *string* or *collective stability* is a much more restrictive criterion than local stability. The regime of string instability can be further divided into a region of convective instability where perturbations grow but finally are convected out of the system (cf., e.g., Fig. 2 below), and a region of absolute instability.

In this contribution, we investigate, by means of simulation, the influence of (i) reaction times, (ii) acceleration capabilities, (iii) temporal anticipation, and (iv) multi-vehicle look-ahead on the stability of traffic flow. We discuss how the influencing factors mentioned above change local stability, string stability, and the limits where the traffic flow is accident-free.

In the following section, we present the models used for the simulation. The Intelligent Driver Model (IDM) (16) will be used as instantaneous nonlinear controller representing the characteristics of automated driving. Its sensitivity is characterized by the acceleration parameter  $\alpha$ . The recently proposed Human Driver Model (HDM) (18) is based on the IDM and implements the additional human-specific properties (reaction times and anticipations) in a systematic way. Later on, we give the results and show how each of the effects mentioned above influences the traffic dynamics. With a suitable anticipation, we obtained string stability for reaction times exceeding the ‘safety time gap’, which, to our knowledge, has not yet been obtained for any other car-following model. Furthermore, we show how the different influences of reaction time and acceleration capability on local and string stability lead to an optimal *range* of the acceleration parameter  $\alpha$  rather than a lower limit as proposed in the literature up to now. Finally, we simulate, for the first time, distributed (i.e., varying) reaction times. We conclude with a discussion of the results.

### MICROSCOPIC TRAFFIC MODEL WITH TIME DELAY AND ANTICIPATION

Most microscopic traffic models describe the instantaneous acceleration and deceleration of each individual ‘driver-vehicle unit’ as a function of the distance and velocity difference to the vehicle in front and on the own velocity (3). The subclass of time-continuous microscopic models (car-following models) is of the general form

$$\frac{dv_\alpha}{dt} = a^{\text{mic}}(s_\alpha, v_\alpha, \Delta v_\alpha), \quad (1)$$

where the own velocity  $v_\alpha$ , the net distance  $s_\alpha$ , and the velocity difference  $\Delta v_\alpha$  to the leading vehicle serve as stimuli determining the acceleration  $a^{\text{mic}}$ . This class of basic models is characterized by (i) instantaneous reaction, (ii) reaction only to the immediate predecessor, and (iii) infinitely exact estimating capabilities of drivers regarding the input stimuli  $s$ ,  $v$ , and  $\Delta v$ , which also means that there are no fluctuations, i.e., drivers react always the same to the same stimuli. In some sense, such models describe driving behavior similar to adaptive cruise control (ACC) systems (10,11).

In the context of control theory, the acceleration is the action to bring (i) the own velocity  $v_\alpha$  towards the desired velocity  $v_0$  if there is no obstruction from other vehicles, and to the velocity  $v_{\alpha-1}$  of the predecessor otherwise, (ii) the observed distance  $s_\alpha$  towards the equilibrium distance  $s_e(v_{\alpha-1})$ . Of course, this condition is only relevant in case of obstruction. For models of the form (1), the equilibrium distance function  $s_e(v)$  is given by

$$a^{\text{mic}}(s_e, v, 0) = 0. \quad (2)$$

In general, the control function  $a^{\text{mic}}$  is strongly nonlinear, and there is a smooth transition

from the control targets for unobstructed traffic to that of obstructed traffic. Notice that ‘obstructed traffic’ (i.e., it is not possible to drive at the desired velocity) does not necessarily mean ‘congested traffic’.

In the following, we introduce the Intelligent Driver Model (IDM) (16), which is a simple car-following model with intuitive parameters. Furthermore, we present three aspects of human driving behavior: (i) finite reaction times, (ii) temporal anticipation, and (iii) looking several vehicles ahead (spatial anticipation). These extensions are formulated in a systematic way and apply to all underlying models of the form (1) (18).

### The Intelligent Driver Model (IDM)

The IDM acceleration of each vehicle  $\alpha$  is a continuous function of the velocity  $v_\alpha$ , the net distance gap  $s_\alpha$ , and the velocity difference (approaching rate)  $\Delta v_\alpha$  to the leading vehicle:

$$\frac{dv_\alpha}{dt} = a \left[ 1 - \left( \frac{v_\alpha}{v_0} \right)^4 - \left( \frac{s^*(v_\alpha, \Delta v_\alpha)}{s_\alpha} \right)^2 \right]. \quad (3)$$

The IDM acceleration consists of a free acceleration  $\dot{v}^{\text{free}} = a[1 - (v/v_0)^4]$  (with  $\dot{v}$  indicating the time derivative) for approaching the desired velocity  $v_0$  with an acceleration slightly below  $a$ , and the braking interaction  $\dot{v}^{\text{int}} = -a(s^*/s)^2$ , where the actual gap  $s_\alpha$  is compared with the ‘desired minimum gap’

$$s^*(v, \Delta v) = s_0 + vT + \frac{v\Delta v}{2\sqrt{ab}}, \quad (4)$$

which is specified by the sum of the minimum distance  $s_0$ , the velocity-dependent safety distance  $vT$  corresponding to the time gap  $T$ , and a dynamic part. The dynamic part implements an accident-free ‘intelligent’ braking strategy that, in nearly all situations, limits braking decelerations to the ‘comfortable deceleration’  $b$ . Notice that all five IDM parameters have an intuitive meaning. The parameters used henceforth (unless stated otherwise) are listed in Table 1. By an appropriate scaling of space and time, the number of parameters can be reduced from five to three.

The IDM has been calibrated to empirical data of several German freeways (16). On a more microscopic level, the IDM was tested together with other microscopic models (19). While all models showed large residual errors, the IDM was one of the best. Furthermore, using the same parameters as in Table 1 (apart from obvious changes for the desired velocity) both the simulated acceleration behaviour from a standstill and deceleration behaviour to a standstill were remarkably close to empirical observations, cf. (20) and (21).

### Finite Reaction Time

A reaction time  $T'$  is implemented simply by evaluating the right-hand side of Eq. (1) at time  $t - T'$ . If  $T'$  is not a multiple of the update time interval, we propose a linear interpolation according to

$$x(t - T') = \beta x_{t-n-1} + (1 - \beta) x_{t-n}, \quad (5)$$

where  $x$  denotes any quantity on the right-hand side of Eq. (1) such as  $s_\alpha$ ,  $v_\alpha$ , or  $\Delta v_\alpha$ , and  $x_{t-n}$  denotes this quantity taken  $n$  time steps before the actual step. Here,  $n$  is the integer part of  $T'/t$ , and the weight factor of the linear interpolation is given by  $\beta = T'/t - n$ . We emphasize that *all* input stimuli  $s_\alpha$ ,  $v_\alpha$ , and  $\Delta v_\alpha$  are evaluated at the delayed time.

Notice that the reaction time  $T'$  is sometimes set equal to the safety time gap  $T$ . However, it is essential to distinguish between these times conceptually. While the time gap  $T$  is a characteristic parameter of the driving style, the reaction time  $T'$  is essentially a physiological parameter and, consequently, at most weakly correlated with  $T$ . We point out that both the time gap  $T$  and the reaction time  $T'$  are to be distinguished from the numerical update time step  $\tau$ , which is sometimes erroneously interpreted as a reaction time as well.

### Temporal Anticipation

We will assume that drivers are aware of their finite reaction time and anticipate the traffic situation accordingly. Besides anticipating the future distance (13), we will anticipate the future velocity using a *constant-acceleration heuristics*. The combined effects of a finite reaction time, and temporal anticipation lead to the following input variables for the underlying car-following model (1):

$$\frac{dv_\alpha}{dt} = \dot{v}^{\text{mic}}(s'_\alpha, v'_\alpha, \Delta v'_\alpha) \quad (6)$$

with

$$s'_\alpha(t) = [s_\alpha - T' \Delta v_\alpha]_{t-T'}, \quad (7)$$

$$v'_\alpha(t) = [v_\alpha + T' \dot{v}_\alpha]_{t-T'}, \quad (8)$$

and

$$\Delta v'_\alpha(t) = \Delta v_\alpha(t - T'). \quad (9)$$

Notice that in Eq. (8) the time delay occurs in the acceleration  $\dot{v}$  as the highest derivative, i.e., the linearized model is of *neutral type*. We did not apply the *constant-acceleration heuristics* for the anticipation of the future velocity difference, or the future distance, as the accelerations of other vehicles cannot be estimated reliably by human drivers. Instead, we have applied the simpler constant-velocity heuristics for these cases. Notice that the proposed heuristics are parameter-free.

These ‘anticipative’ terms include derivative quantities (the accelerations), and velocity differences. In the framework of control theory, they act as nonlinear derivative elements in the control path.

### Spatial Anticipation for Several Vehicles Ahead

Let us now split up the acceleration of the underlying microscopic model into a single-vehicle acceleration on a nearly empty road depending on the considered vehicle  $\alpha$  only, and a braking deceleration taking into account the vehicle-vehicle interaction with the preceding vehicle:

$$\dot{\mathbf{v}}^{\text{mic}}(s_\alpha, v_\alpha, \Delta v_\alpha) := \dot{\mathbf{v}}_\alpha^{\text{free}} + \dot{\mathbf{v}}^{\text{int}}(s_\alpha, v_\alpha, \Delta v_\alpha). \quad (10)$$

This splitting up is motivated by the concept of a ‘social force model’ which is underlying the IDM and the HDM. In this concept there are several forces such as a ‘driving force’ to accelerate to the desired velocity and repulsive forces caused by the front vehicles (18). Next, we model the reaction to several vehicles ahead just by summing up the corresponding vehicle-vehicle pair interactions  $\dot{\mathbf{v}}_\beta^{\text{int}}$  from vehicle  $\beta$  to vehicle  $\alpha$  for the  $n_\alpha$  nearest preceding vehicles  $\beta$ :

$$\frac{d\mathbf{v}_\alpha}{dt} = \dot{\mathbf{v}}_\alpha^{\text{free}} + \sum_{\beta=\alpha-n_\alpha}^{\alpha-1} \dot{\mathbf{v}}_{\alpha\beta}^{\text{int}}, \quad (11)$$

where all distances, velocities and velocity differences on the right-hand side are given by Eqs. (7) – (9). Each pair interaction between vehicle  $\alpha$  and vehicle  $\beta$  is specified by

$$\dot{\mathbf{v}}_{\alpha\beta}^{\text{int}} = \dot{\mathbf{v}}(s_{\alpha\beta}, v_\alpha, v_\alpha - v_\beta), \quad (12)$$

where

$$s_{\alpha\beta} = \sum_{j=\beta+1}^{\alpha} s_j \quad (13)$$

is the sum of all *net* gaps between the vehicles  $\alpha$  and  $\beta$ . For the IDM, there exists a closed-form solution of the multi-anticipative equilibrium distance as a function of the velocity. Notice that in the limiting case of anticipation to arbitrary many vehicles we obtain  $\lim_{n_\alpha \rightarrow \infty} \gamma(n_\alpha) = \pi/\sqrt{6} = 1.283$  for the IDM. This means that the combined effects of all non-nearest-neighbor interactions would lead to an increase of the equilibrium distance by just about 28% (18).

In summary, the HDM consists of all extensions of the underlying car-following model described in the sections above. The HDM was tested against empirical one-minute data of German freeways (18) and it was found that it described the observed spatiotemporal structures of congested traffic. Particularly, the transitions between free and congested traffic were smoother than in the IDM, in agreement with the empirical results.

## MICROSCOPIC TRAFFIC SIMULATIONS OF VEHICLE PLATOONS

We investigate the string stability by simulating a platoon of vehicles following an externally controlled lead vehicle. As initial conditions, we assume the platoon to be in equilibrium, i.e., the initial velocities of all platoon vehicles are equal to  $v_{\text{lead}}$  and the gaps equal to  $s_e(v_{\text{lead}})$ , cf. Eq. (2), so that the initial model accelerations are equal to zero.

The externally controlled vehicle drives at  $v_{\text{lead}} = 25$  m/s for the first 1000 s, before it decelerates with  $-2$  m/s<sup>2</sup> for 3 s, which is a realistic scenario in daily traffic situations. This braking maneuver reduces the velocity to  $v_{\text{lead}} = 19$  m/s, which is kept constant until the simulation ends at  $t = 2500$  s. This braking maneuver serves as *perturbation* for all simulations throughout this paper. Notice that the nonlinear dynamics resulting from this *finite* perturbation cannot be handled by linearization anymore.

In all simulations, we have used an explicit integration scheme assuming constant accelerations between each update time interval  $\Delta t$  according to

$$\begin{aligned} v_\alpha(t + \Delta t) &= v_\alpha(t) + \dot{v}_\alpha(t)\Delta t, \\ x_\alpha(t + \Delta t) &= x_\alpha(t) + v_\alpha(t)\Delta t + \frac{1}{2}\dot{v}_\alpha(t)(\Delta t)^2 \end{aligned} \quad (14)$$

The update time interval is set to  $\Delta t = 0.1$  s. We will use the IDM parameters given in Table 1 unless stated otherwise. If  $n_\alpha$  is larger than the number of preceding vehicles (which can happen for the first vehicles of the platoon) then  $n_\alpha$  is reduced accordingly. Furthermore, we restrict the maximum braking deceleration to  $9 \text{ m/s}^2$ , which is the physical limit on dry roads.

### Stability Boundaries for a Platoon of Vehicles

We distinguish three stability regimes: (i) *string stability*, i.e., all perturbations introduced by the deceleration of the lead vehicles are damped away, (ii) an *oscillatory regime*, where perturbations increase but do not lead to collisions, and (iii) an *instability with accidents*. The condition for a simulation to be in the crash regime (iii) is fulfilled if there is *some* time  $t$  and *some* vehicle  $\alpha$  so that  $s_\alpha(t) < 0$ . The condition for string stability is fulfilled if  $|\dot{v}_\alpha(t)| < 3 \text{ m/s}^2$  at *all* times (including the period where the leading vehicle decelerates) and for *all* vehicles. Additionally, string stability requires that, for sufficiently long times after the braking maneuver, the accelerations of *all* vehicles converge to zero. Finally, if neither the conditions for the crash regime nor that for the stable regime are fulfilled, the simulation result is attributed to the oscillatory regime.

Figure 3 shows the three stability regimes as a function of the reaction time  $T'$  and the platoon size  $n$  for the following simulation scenarios:

1. The first scenario with neither spatial anticipation ( $n_a = 1$ ) nor temporal anticipation serves as reference. This case corresponds to the conventional IDM car-following model with finite reaction time. A platoon of 100 vehicles is stable for reaction times of up to  $T'_{c1} = 0.9$  s. Test runs with larger platoon sizes (up to 1000 vehicles) did not result in different thresholds suggesting that stability for a platoon size of 100 essentially means string stability for arbitrarily large platoon sizes. For reaction times  $T' > T'_{c2} = 1.15$  s, the collective instability leads to accidents, at least, when limiting the braking deceleration to  $9 \text{ m/s}^2$ .
2. The second scenario extends the reference scenario by implementing the parameter-free temporal anticipation. While the stability limit,  $T'_{c1} = 0.95$  s, is only slightly increased with respect to scenario (1), the collision limit  $T'_{c2} = 1.4$  s is increased significantly.
3. The third simulation scenario implements the spatial anticipation by looking  $n_a = 4$  vehicles ahead as extension compared to the reference case  $n_a = 1$ . This spatial anticipation increases the stability and shifts both boundaries,  $T'_{c1}$  and  $T'_{c2}$  to significantly higher values.
4. The fourth scenario combines temporal and spatial anticipation ( $n_a = 4$ ), which leads to the

most stable system. Particularly, the second boundary is shifted to values of  $T'_{c2} \geq 2$  s.

Remarkably, the simulation shows that, with a suitable anticipation, we could obtain collision-free traffic for reaction times exceeding the safety time gap of  $T = 1.5$  s. Further increasing the number of anticipated vehicles  $n_a$  does not change the thresholds significantly.

So far, we have assumed constant and identical reaction times  $T'_\alpha = T'$  for all vehicles  $\alpha$  in the simulation. Since the human reaction time varies strongly depending on the concrete situation and between different persons (5), we also investigate the role of *distributed reaction times*, i.e., every driver has a different reaction time  $T'_\alpha$  with the mean value  $\langle T'_\alpha \rangle = T'$ . To this end, we generalize the concept of linear interpolation of Eq. (5) to individual delays for each driver-vehicle unit  $\alpha$ .

Figure 4 shows the simulation results for several simulation runs for the reference scenario (1) without anticipation and the scenario (4) with temporal and spatial anticipation. The reaction time has been uniformly distributed within a range of  $\pm 30\%$  around the mean value. Interestingly, the phase boundary  $T'_{c1}$  between the stable and oscillatory regime is nearly not affected by the variation of the reaction time. The phase boundary  $T'_{c2}$  for the fourth scenario is even slightly shifted towards higher stability for platoon sizes of  $n \geq 70$  vehicles. However, the critical value  $T'_{c1}$  is slightly reduced when dealing with non-identical reaction times. In summary, distributed reaction times have a remarkably low influence on the stability of traffic flow. In particular, the expected stability increased by destructive interference of the different eigenfrequencies of the observations has not been observed.

### Role of Vehicle Acceleration

As mentioned in the introduction, there are basically two different sources of instability for traffic flow: The finite reaction time modelled by the HDM parameter  $T'$ , and finite acceleration capabilities modelled by the IDM parameter  $\alpha$ , which gives the maximum acceleration. Clearly, stability always decreases when  $T'$  increases. In this subsection, we investigate how the acceleration parameter  $\alpha$  influences the instability mechanisms and come to the remarkable result that stability reaches its maximum for a certain range of values for  $\alpha$  (that depends on  $T'$ ). Traffic flow becomes more unstable if the value of  $\alpha$  is higher *or* lower than this range.

Figure 2 (left column) shows time series of the acceleration of some selected vehicles for scenario (1) with  $T' = 0.9$  s, and the acceleration parameter changed from  $2 \text{ m/s}^2$  to the approximately 'optimal' value  $1 \text{ m/s}^2$ . The system is string stable: the initial perturbation of  $2 \text{ m/s}^2$  dissipates quickly. In the right column of Fig. 2, the acceleration parameter is lowered from  $1 \text{ m/s}^2$  to  $\alpha = 0.3 \text{ m/s}^2$ . The effect is as expected (16,17): The initial perturbation decreases for the first few vehicles (the system is locally stable), before it increases again for the next vehicles, and finally leads to a traffic breakdown in the neighborhood of vehicle 100 at a simulated time  $t \approx 1250$  s: The system is string unstable. After the first breakdown, further stop-and-go waves develop (not shown here).

Remarkably, the system becomes unstable as well when *increasing* the acceleration capability from the reference value  $1 \text{ m/s}^2$  to  $\alpha = 2.5 \text{ m/s}^2$  as shown in Fig. 5. The instability mechanism, however, is different. For low values of  $\alpha$ , the traffic breakdown is initially triggered

by a long-wavelength instability as can be seen in the plots for the cars 10 and 50 of Fig. 2 (right column), before additional shorter oscillations appear immediately before the breakdown (vehicles 80 and 100). In contrast, the initial instability for high values of  $\alpha$  has its maximum growth rates at shorter frequencies (of about 4 s), which can be seen from Fig. 5 for the vehicle sequence 4, and 50 leading to the first stop-and-go wave, and the sequence 50, 70, leading to the second one. Further stop-and-go waves develop at later times for vehicles further upstream. Interestingly, the period of the resulting stop-and-go waves is about the same for the high-wavelength, and low-wavelength mechanisms to instability.

## DISCUSSION AND CONCLUSIONS

In this contribution, we have investigated two causes for the instability of traffic flow, the time lag caused by finite accelerations of the vehicles, and the delay caused by the finite reaction time of the drivers. Furthermore, we have simulated to which degree drivers may compensate for these delays by looking several vehicles ahead and anticipate future traffic situations.

Since vehicular traffic flow is a multi-particle system with many degrees of freedom, two concepts of linear stability have to be considered: Local stability of a car following a leader that drives at constant velocity, and string or collective stability of a platoon of several vehicles following each other. Typically, string stability is a much more restrictive criterion than local stability.

Our main results are: (i) By means of simulation, we determined the string stability boundaries as a function of the reaction time  $T'$  for a variable platoon size of vehicles. With a suitable spatial and temporal anticipation, we obtained string stability for reaction times near the safety time gap, which, to date, has not yet been obtained for any other car-following model. (ii) When varying the maximum acceleration capability, we come to the remarkable result that stability reaches its maximum for a certain range of values for  $\alpha$  (that depends on the reaction time  $T'$ ). Traffic flow becomes more unstable if the value of the maximum acceleration is higher or lower than this value. This can be understood by the interplay between the two mechanisms to instabilities: If the value of  $T'$  and  $\alpha$  are both comparatively high, then the ratio between the reaction time and the time scale  $\tau \approx v_0 / \alpha$  of velocity changes is high leading to instabilities on the level of individual vehicles. Conversely, for low values of  $\alpha$ , the lag time scale  $\tau$  itself leads to the well-known collective instabilities already observed for zero reaction time. (iii) Distributed reaction times, i.e., every driver has a different reaction time, can stabilize the system compared to drivers with identical reaction times that are equal to the mean. Generally, however, the effect introduced by the heterogeneity among drivers is small.

We checked if these results are robust with respect to parameter changes and found no qualitative difference for other parameter sets within a reasonable range. For example, when changing the time gap from  $T = 1.5$  s to  $T = 0.9$  s (cf. the Introduction), the stability thresholds  $T'_{c1}$  and  $T'_{c2}$  reduce proportionally, i.e.,  $T'_{c1}$  remains typically of the order of or slightly below  $T$  while  $T'_{c2} > T$ . Preliminary results show that the results are also robust when applying the HDM to other car-following models.

## ACKNOWLEDGMENTS

The authors would like to thank Dr. H.-J. Stauss for the excellent collaboration and the Volkswagen AG for partial financial support within the BMBF project INVENT.

## REFERENCES

1. Brackstone, M., and M. McDonald. Car-following: A historical review. *Transportation Research F*, Vol. 2, 1999, pp. 181–196.
2. Holland, E., 1998. A generalised stability criterion for motorway traffic. *Transportation Research B*, Vol. 32, 1998, pp. 141–154.
3. Helbing, D. Traffic and related self-driven many-particle systems. *Reviews of Modern Physics*, Vol. 73, 2001, pp. 1067–1141.
4. Shiffrin, R., and W. Schneider. Controlled and automatic human information processing ii: Perceptual learning, automatic attending, and a general theory. *Psychological Review*, Vol. 84, 1977, pp. 127–190.
5. Green, M. ‘How long does it take to stop?’ Methodological analysis of driver perception-brake times. *Transportation Human Factors*, Vol. 2, 2000, pp. 195–216.
6. Tilch, B., and D. Helbing. Evaluation of single vehicle data in dependence of the vehicle-type, lane, and site. In: Helbing, D., H. Herrmann, M. Schreckenberg, and D. Wolf (Eds.), *Traffic and Granular Flow '99*. Springer, Berlin, 2000, pp. 333–338.
7. Knospe, W., L. Santen, A. Schadschneider, and M. Schreckenberg. Single-vehicle data of highway traffic: Microscopic description of traffic phases. *Phys. Rev. E*, Vol. 65, 2002, p. 056133.
8. Newell, G. Nonlinear effects in the dynamics of car following. *Operations Research*, Vol. 9, 1961, p. 209.
9. Bando, M., K. Hasebe, A. Nakayama, A. Shibata, and Y. Sugiyama. Dynamical model of traffic congestion and numerical simulation. *Phys. Rev. E*, Vol. 51, 1995, pp. 1035–1042.
10. Kesting, A., M. Treiber, M. Schönhof, and D. Helbing. Extending adaptive cruise control (ACC) towards adaptive driving strategies. Paper number 07-306. In: *Proceedings of the TRB Annual Meeting*. TRB, National Research Council, Washington, D.C., 2007. Accepted for publication in *Transportation Research Record: Journal of the Transportation Research Board*.
11. Kesting, A., M. Treiber, M. Schönhof, F. Kranke, and D. Helbing. Jam-avoiding adaptive cruise control (ACC) and its impact on traffic dynamics. In: *Traffic and Granular Flow '05*. Springer, Berlin, 2007, pp. 633–643. e-print [physics/0601096](http://physics/0601096).
12. Bando, M., K. Hasebe, K. Nakanishi, and A. Nakayama. Analysis of optimal velocity model with explicit delay. *Phys. Rev. E*, Vol. 58, 1998, p. 5429.
13. Davis, L. Modifications of the optimal velocity traffic model to include delay due to driver reaction time. *Physica A*, Vol. 319, 2002, p. 557.
14. Brogan, W. L. *Modern control theory*. Prentice-Hall, Upper Saddle River, USA, 1991.
15. Isidori, A. *Nonlinear Control Systems*. Springer, New York, 1995.
16. Treiber, M., A. Hennecke, and D. Helbing. Congested traffic states in empirical observations and microscopic simulations. *Phys. Rev. E*, Vol. 62, 2000, pp. 1805–1824.
17. Treiber, M., A. Hennecke, and D. Helbing. Derivation, properties, and simulation of a gas-kinetic-based, non-local traffic model. *Phys. Rev. E*, Vol. 59, 1999, pp. 239–253.
18. Treiber, M., A. Kesting, and D. Helbing. Delays, inaccuracies and anticipation in microscopic traffic models. *Physica A*, Vol. 360, 2006, pp. 71–88.
19. Brockfeld, E., R. Kühne, and P. Wagner. Calibration and validation of microscopic traffic models. In *Transportation Research Record: Journal of the Transportation Research Board*, No. 1876, TRB, National Research Council, Washington, D.C., 2004, pp. 62–70.

20. Wang, J., K. Dixon, H. Li, and J. Ogle. Normal acceleration behaviour of passenger vehicles starting from rest at all-way stop-controlled intersections. In *Transportation Research Record: Journal of the Transportation Research Board, No. 1883*, TRB, National Research Council, Washington, D.C., 2004, pp. 158–166.
21. Wang, J., K. Dixon, H. Li, and J. Ogle. Normal deceleration behaviour of passenger vehicles at stop sign-controlled intersections. In *Transportation Research Record: Journal of the Transportation Research Board, No. 1937*, TRB, National Research Council, Washington, D.C., 2005, pp. 120–127.

**TABLE 1** Parameters of the Intelligent Driver Model (IDM) with the values used in this paper unless stated otherwise. The IDM is used together with an explicit reaction time  $T'$ , temporal anticipation, and spatial anticipation. The vehicle length is 5 m. Furthermore, we restrict the maximum braking deceleration to  $9 \text{ m/s}^2$  as the physical limit on dry roads.

**FIGURE 1** Flow diagram of the elements of the nonlinear feedback loop representing the actions of the driver and the vehicle dynamics.

**FIGURE 2** Time series of the acceleration for selected platoon vehicles for simulations with the IDM parameter for the maximum acceleration set to  $\alpha = 1 \text{ m/s}^2$  (left column), and  $\alpha = 0.3 \text{ m/s}^2$  (right column). In both cases, the reaction time is  $T' = 0.9 \text{ s}$ , and the drivers use temporal anticipation but no spatial anticipation ( $n_a = 1$ ). The first vehicle induces a perturbation due to the braking maneuver at  $t = 1000 \text{ s}$ . For  $\alpha = 1 \text{ m/s}^2$ , the is string stable, while it is unstable for  $\alpha = 0.3 \text{ m/s}^2$ .

**FIGURE 3** String stability regimes of a platoon of identical vehicles as a function of the platoon size and the reaction time  $T'$  for the scenarios (1) - (4) described in the text. The graph (a) depicts scenario (1) assuming conventional follow-the-leader behavior ( $n_a = 1$ ) without temporal anticipation; (b) with temporal anticipation ( $n_a = 1$ ) (scenario (2)); (c) reaction to  $n_a = 4$  vehicles without temporal anticipation (scenario (3)); (d) reaction to  $n_a = 4$  vehicles with temporal anticipation (scenario (4)). In the diagrams (b)-(d), the first scenario of graph (a) is plotted with thin lines for purposes of comparison. The externally controlled first vehicle induced a finite perturbation. In the ‘stable’ phase, all perturbations are damped away. In the oscillatory regime, the perturbations increase, but do not lead to collision.

**FIGURE 4** String stability regimes of a platoon of vehicles  $\alpha$  with different individual reaction times for three simulation runs with different random seeds. The reaction time  $T'_\alpha$  has been distributed uniformly within 30% around the mean value  $\langle T'_\alpha \rangle = T'$ . The diagram (a) refers to the scenario (1) with neither temporal nor spatial anticipation, while the diagram (b) corresponds to the fourth scenario with temporal and spatial anticipation ( $n_a = 4$ ). The thin lines display the phase boundaries for identical reaction times. The variation of the reaction times leads to a remarkably unchanged stability boundary  $T'_{c1}$  between the stable and oscillating regime. The critical boundary  $T'_{c2}$  is even slightly increased for some platoons, see (b).

**FIGURE 5** Time series of the acceleration for the same scenario as in Fig. 2, but the IDM parameter for the maximum acceleration is increased to  $\alpha = 2.5 \text{ m/s}^2$ . Again, the first vehicle induces a perturbation due to the braking maneuver at  $t = 1000 \text{ s}$  (not shown here). The increased acceleration parameter  $\alpha$  in combination with the delayed reaction causes higher frequencies with periods about 4 s that finally trigger stop-and-go-waves of a much higher period (about 50 s).

**TABLE 1 Parameters of the Intelligent Driver Model (IDM) with the values used in this paper unless stated otherwise. The IDM is used together with an explicit reaction time  $T'$ , temporal anticipation, and spatial anticipation. The vehicle length is 5 m. Furthermore, we restrict the maximum braking deceleration to  $9 \text{ m/s}^2$  as the physical limit on dry roads.**

Parameter	Value
Desired velocity $v_0$	120 km/h
Safety time gap $T$	1.5 s
Jam distance $s_0$	2 m
Maximum acceleration $a$	$2.0 \text{ m/s}^2$
Desired deceleration $b$	$2.0 \text{ m/s}^2$

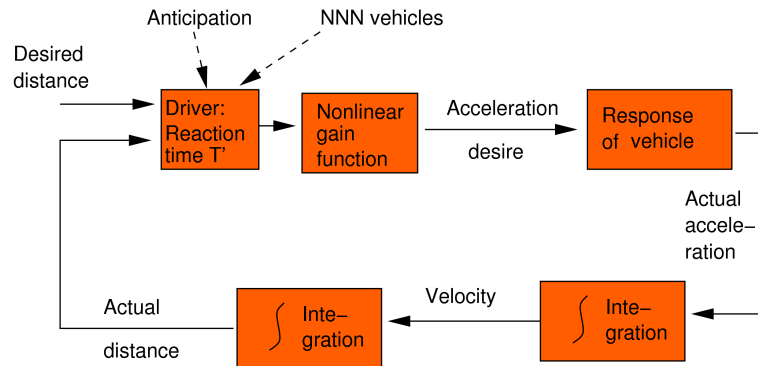


**FIGURE 1** Flow diagram of the elements of the nonlinear feedback loop representing the actions of the driver and the vehicle dynamics.

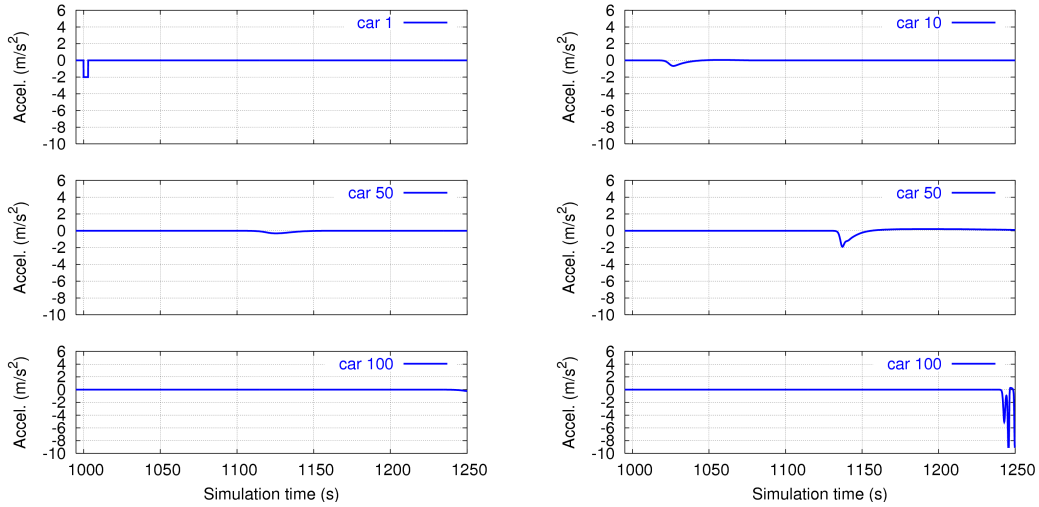


**FIGURE 2** Time series of the acceleration for selected platoon vehicles for simulations with the IDM parameter for the maximum acceleration set to  $\alpha = 1 \text{ m/s}^2$  (left column), and  $\alpha = 0.3 \text{ m/s}^2$  (right column). In both cases, the reaction time is  $T' = 0.9 \text{ s}$ , and the drivers use temporal anticipation but no spatial anticipation ( $n_a = 1$ ). The first vehicle induces a perturbation due to the braking maneuver at  $t = 1000 \text{ s}$ . For  $\alpha = 1 \text{ m/s}^2$ , the string is stable, while it is unstable for  $\alpha = 0.3 \text{ m/s}^2$ .

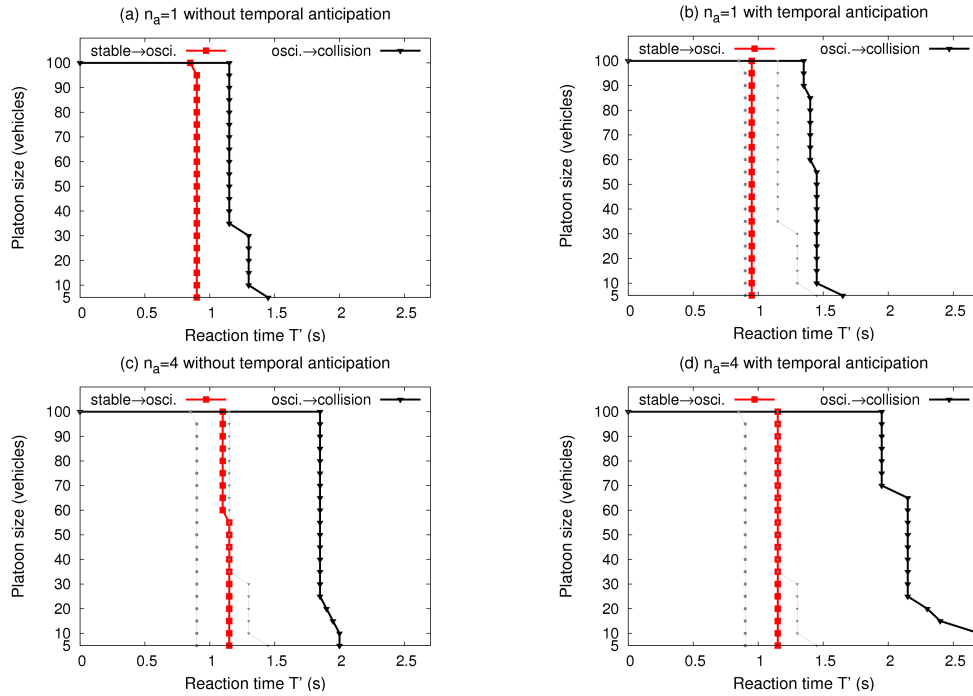


**FIGURE 3** String stability regimes of a platoon of identical vehicles as a function of the platoon size and the reaction time  $T'$  for the scenarios (1) - (4) described in the text. The graph (a) depicts scenario (1) assuming conventional follow-the-leader behavior ( $n_a = 1$ ) without temporal anticipation; (b) with temporal anticipation ( $n_a = 1$ ) (scenario (2)); (c) reaction to  $n_a = 4$  vehicles without temporal anticipation (scenario (3)); (d) reaction to  $n_a = 4$  vehicles with temporal anticipation (scenario (4)). In the diagrams (b)-(d), the first scenario of graph (a) is plotted with thin lines for purposes of comparison. The externally controlled first vehicle induced a finite perturbation. In the 'stable' phase, all perturbations are damped away. In the oscillatory regime, the perturbations increase, but do not lead to collision.

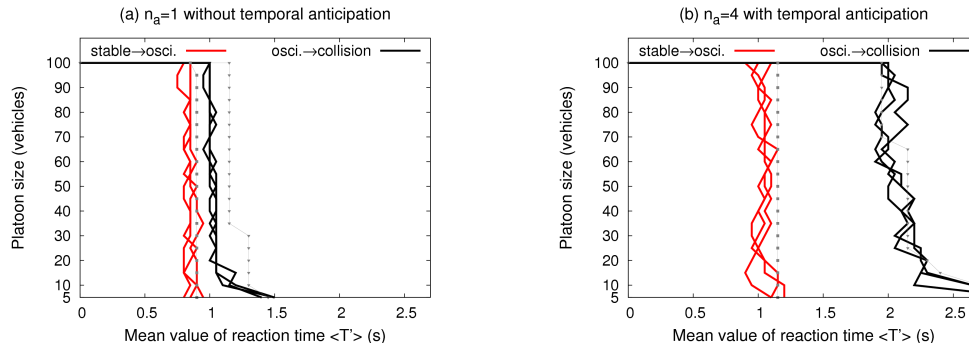


**FIGURE 4** String stability regimes of a platoon of vehicles  $\alpha$  with different individual reaction times for three simulation runs with different random seeds. The reaction time  $T'_\alpha$  has been distributed uniformly within 30% around the mean value  $\langle T'_\alpha \rangle = T'$ . The diagram (a) refers to the scenario (1) with neither temporal nor spatial anticipation, while the diagram (b) corresponds to the fourth scenario with temporal and spatial anticipation ( $n_a = 4$ ). The thin lines display the phase boundaries for identical reaction times. The variation of the reaction times leads to a remarkably unchanged stability boundary  $T'_{c1}$  between the stable and oscillating regime. The critical boundary  $T'_{c2}$  is even slightly increased for some platoons, see (b).

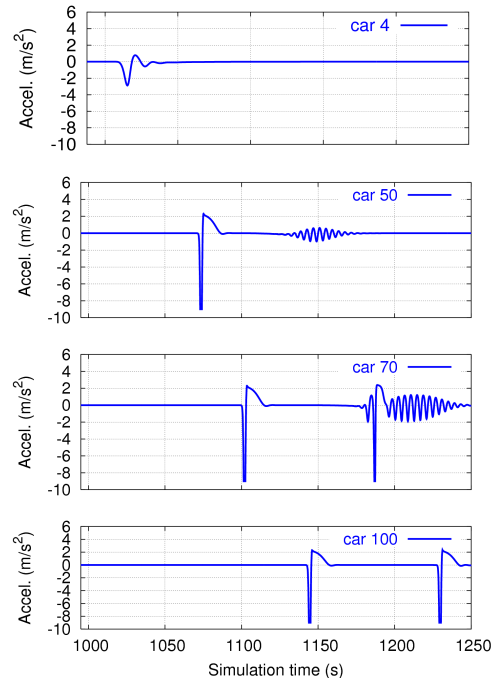


**FIGURE 5** Time series of the acceleration for the same scenario as in Fig. 2, but the IDM parameter for the maximum acceleration is increased to  $a = 2.5 \text{ m/s}^2$ . Again, the first vehicle induces a perturbation due to the braking maneuver at  $t = 1000 \text{ s}$  (not shown here). The increased acceleration parameter  $a$  in combination with the delayed reaction causes higher frequencies with periods about 4 s that finally trigger stop-and-go-waves of a much higher period (about 50 s).